



# HHS Public Access

Author manuscript

*ACS Chem Neurosci.* Author manuscript; available in PMC 2020 April 17.

Published in final edited form as:

*ACS Chem Neurosci.* 2019 April 17; 10(4): 1908–1914. doi:10.1021/acschemneuro.8b00265.

## Stress-induced alterations of norepinephrine release in the bed nucleus of the stria terminalis of mice

Karl T. Schmidt<sup>1</sup>, Viren H. Makhijani<sup>1,2</sup>, Kristen M. Boyt<sup>1</sup>, Elizabeth S. Cogan<sup>1</sup>, Dipanwita Pati<sup>1</sup>, Melanie M. Pina<sup>1</sup>, Isabel M. Bravo<sup>1</sup>, Jason L. Locke<sup>5</sup>, Sara R. Jones<sup>5</sup>, Joyce Besheer<sup>1,2,3</sup>, and Zoé A. McElligott<sup>1,2,3,4,#</sup>

<sup>1</sup>Bowles Center for Alcohol Studies, University of North Carolina at Chapel Hill, Chapel Hill NC, USA, 27599

<sup>2</sup>Neuroscience Curriculum, University of North Carolina at Chapel Hill, Chapel Hill NC, USA, 27599

<sup>3</sup>Department of Psychiatry, University of North Carolina at Chapel Hill, Chapel Hill NC, USA, 27599

<sup>4</sup>Department of Pharmacology, University of North Carolina at Chapel Hill, Chapel Hill NC, USA, 27599

<sup>5</sup>Department of Physiology and Pharmacology, Wake Forest School of Medicine, Winston-Salem, NC, USA, 27157

### Abstract

Stress can drive adaptive changes to maintain survival during threatening stimuli. Chronic stress exposure, however, may result in pathological adaptations. A key neurotransmitter involved in stress signaling is norepinephrine. Previous studies show that stress elevates norepinephrine levels in the bed nucleus of the stria terminalis (BNST), a critical node regulating anxiety and upstream of stress responses. Here, we use mice expressing channelrhodopsin in norepinephrine neurons to selectively activate terminals in the BNST, and measure norepinephrine release with fast-scan cyclic voltammetry. Mice exposed to a single restraint session show an identical norepinephrine release profile compared to that of unexposed mice. Mice experiencing five days of restraint stress, however, show elevated norepinephrine release across multiple stimulation parameters, and reduced sensitivity to the  $\alpha_2$ -adrenergic receptor antagonist idazoxan. These data are the first to examine norepinephrine release in the BNST to tonic and phasic stimulation frequencies, and confirm that repeated stress alters autoreceptor sensitivity.

#Corresponding author: Tel: (919)966-8637, zoemce@email.unc.edu.  
Author Contributions.

Concept and design, Z.A.M. and K.T.S.; K.T.S. responsible for electrode fabrication, FSCV experiments, data analysis, writing the manuscript; V.H.M and J.B. responsible for CORT analysis; K.M.B. responsible for FISH; E.S.C. responsible for tissue collection for FISH and HPLC; D.P. and M.M.P. responsible for electrophysiological recordings; I.M.B participated in stress procedures, electrode fabrication, and FSCV experiments; J.L.L. and S.R.J responsible for HPLC; Z.A.M. responsible for writing the manuscript.

## Keywords

Stress; Norepinephrine; Fast-Scan Cyclic Voltammetry; Optogenetics; Bed Nucleus of the Stria Terminalis; Corticosterone

Stress responses are important physiologic reactions to potentially harmful environmental stimuli. Under some conditions, however, such as chronic stress exposure or especially traumatic events, persistent alterations in the stress response occur, leading to abnormal and potentially maladaptive responses. Previous research has shown a central role of the catecholamine neurotransmitter norepinephrine (NE) in the physiological and behavioral stress responses<sup>1</sup>. NE release, in key downstream nuclei following stress has been implicated in a number of psychological disorders including addiction<sup>2-3</sup>, affective disorders<sup>1</sup>, and PTSD<sup>4</sup>.

Noradrenergic neurons project through two primary pathways in the brain: the dorsal noradrenergic bundle and ventral noradrenergic bundle. The pontine locus coeruleus (A6) gives rise to the dorsal noradrenergic bundle sending projections throughout the cortex, thalamus, hippocampus, cerebellum, and amygdala<sup>5-7</sup>. In contrast, the ventral noradrenergic bundle mainly arises from two nuclei, A1 of the rostral ventrolateral medulla and A2 of the nucleus of the solitary tract<sup>6</sup>, and projects mainly to hypothalamus, parabrachial nucleus, midbrain, and bed nucleus of the stria terminalis (BNST)<sup>3, 6, 8</sup>. Of particular interest is the projection from the medullary noradrenergic nuclei (i.e. A1/A2) to the fusiform nucleus of the ventral BNST because it comprises the densest region of NE terminals in the brain<sup>9-12</sup>, does not receive innervation from dopaminergic neurons<sup>11</sup>, and serves as a critical nucleus for processing affective state<sup>13</sup>. Furthermore, multiple stressors have been shown to increase NE release in the BNST, and blockade of postsynaptic  $\alpha_1$ -adrenergic receptors ( $\alpha_1$ -AR) in the BNST reduced circulating adrenocorticotrophic hormone concentrations and blockade of  $\alpha_1$ - and  $\beta$ ARs reduced anxiety-like behavior<sup>14</sup>. There appears to be a critical role of ARs in the BNST in the response to stress, as chronic restraint stress occludes the expression of  $\alpha_1$ -AR dependent plasticity<sup>15</sup> and multiple adrenergic receptors can drive release of corticotropin releasing factor within the BNST<sup>15-16</sup>.

Previously, we and others have demonstrated that stress exposure modulates norepinephrine release in the BNST in rats<sup>17-18</sup>. Due to innervation of multiple biogenic amine pathways, and a reliance on electrical stimulation, these studies could not be performed at physiologically relevant frequency patterns<sup>19-20</sup>, and it was challenging to isolate catecholamine release from noradrenergic terminals<sup>11</sup>. Here, we use a combination of optogenetics and fast-scan cyclic voltammetry (FSCV) to examine stress-induced alterations in NE release in the ventral BNST. Using a mouse line expressing Cre-recombinase driven by the dopamine-beta-hydroxylase (DBH::Cre) promoter crossed with the Allen Institute's "Ai32" mouse line<sup>21</sup> that expresses channelrhodopsin (ChR2) in a Cre-recombinase dependent manner, we were able to selectively probe noradrenergic release in the ventral BNST using optogenetically-driven stimulation with FSCV following various restraint stress exposure paradigms. We show that repeated restraint stress exposure, but not single stress

exposure, enhances NE release in the BNST of mice. Our data suggests this phenomenon may be driven by alterations in  $\alpha_2$ -AR function.

## Results and Discussion

Before using the DBH::Cre(+/-)::Ai32(+/+) mice to examine stress-induced neuroadaptations, we first characterized the noradrenergic system in this line. Transgene expression did not alter tissue content of NE in the BNST, cortex, striatum, hippocampus, or amygdala as measured by high-performance liquid chromatography (Fig. 1A). Using *ex vivo* patch-clamp electrophysiology, we recorded the activity of ChR2-eYFP<sup>+</sup> cell bodies from the A2 cell group (Fig. 1B) in 300  $\mu$ m coronal slices of the nucleus of the solitary tract. Optical stimulation of these cell bodies evoked action potentials at both low-tonic frequencies (10 pulses, 1 Hz, 4 ms, 490 nm; Fig. 1C) and high-phasic frequencies (15 Hz; Fig. 1D) with complete fidelity (1:1 light pulse to spike ratio, n=5 cells). When examining terminal regions from these cells, we observed a dense fiber projection of noradrenergic neurons in the ventral BNST's fusiform subnucleus (Fig. 1E). Repeated optogenetic stimulations of equal parameters (20 pulses, 10 Hz, 4 ms, 490 nm) applied to slices containing the dense noradrenergic terminals within the ventral BNST with 5 min between each stimulation induced stable NE release with an average peak concentration of 0.1689  $\mu$ M NE at each stimulation (Fig. 1F). This concentration is in line with what was previously measured *in vivo* in rats with supraphysiological frequencies and higher pulse numbers of electrical stimulation at distal sites<sup>11, 18, 22</sup>. Previously reported dopamine release using a DAT::CRE line crossed with Ai32 mice indicated a decrease in optogenetically-evoked dopamine with repeated stimulations in the striatum<sup>23</sup>. As we do not see this consecutive decrease in our recordings, it may be a result of differences in Cre-driver line (as the DAT::Cre line has altered clearance mechanisms), brain region, or catecholamine. Furthermore, we observed stimulation dependent NE release with low concentrations (mean [NE] = 0.037  $\mu$ M; n = 8) detected following a single pulse of light and higher concentrations (mean [NE] = 0.243  $\mu$ M; n = 6) following phasic burst-like (20 pulses, 15 Hz) stimulation (Fig. G, H, I, J).

After validating the utility of the DBH::Cre(+/-)::Ai32(+/+) line to study the release and uptake of NE in the vBNST, we next tested the hypothesis that *in vivo* stress exposure would engage norepinephrine neurons and elicit a stress response. We exposed mice on the same background to one of three conditions: stress naïve, single 2-hour restraint stress exposure, or repeated 5 days, 2-hour restraint stress exposure. Immediately following a restraint stress session, we collected trunk blood and analyzed it for plasma corticosterone (CORT) concentrations. As anticipated, restraint stress exposure significantly elevated CORT, and, as reported previously<sup>24-25</sup>, this CORT response was sensitive to habituation (Fig. 2A). Simultaneously, we retrieved the brains from these mice and used dual fluorophore fluorescent *in situ* hybridization (FISH) to probe for *cFos* and *DBH* mRNA in the nucleus of solitary tract. Both a single restraint stress and repeated stress increased *cFos* transcription in the A2 NE neurons (Fig. 2B & C). These data show that our stress paradigm stimulates activity in NE neurons and acutely engages the hypothalamic pituitary adrenal stress axis. Interestingly, whereas the restraint enhancement of the CORT response habituated to repeat exposure to restraint stress, the noradrenergic neurons of the nucleus of the solitary tract (i.e.

A2) maintained an increased activation following multiple restraint sessions. These data suggest that the central nervous system stress response and the peripheral stress response may have separate activation mechanisms following repeated restraint stress.

We next hypothesized that these stress paradigms would engage plasticity within the noradrenergic system, as we and others have previously observed using different stressors in rat<sup>17-18</sup>. To test this hypothesis, we performed *ex vivo* slice optogenetics-assisted FSCV to measure NE release from terminals in the BNST of mice following our stress conditions: naïve, single restraint, and 5 days of restraint. In contrast to the CORT and *cFos* studies, all FSCV recordings occurred on the day immediately following the final stress exposure to examine an adaptive response. Our stimulation parameters examined light pulses (4ms duration) to various frequency (20 pulses at 1, 2, 5, 10, 15 Hz) and pulse number (1, 2, 5, 10, 20 pulses at 5 Hz or 10 Hz) protocols, and were chosen to encapsulate a range of physiologically relevant noradrenergic firing patterns<sup>26-28</sup>. Repeated restraint stress exposure significantly increased NE release across the range of stimulation frequencies with the largest differences observed at high phasic frequencies (Fig. 3A). Stress naïve and single stress exposed animals did not significantly differ from one another. Similar results were observed with 5 Hz (Fig. 3B) and 10 Hz (Fig. 3C) phasic stimulations with the larger differences observed with increased pulses (approximately 3.3- to 5-fold difference following repeated stress exposure as compared to naïve and single stress conditions).

Finally, in order to examine whether autoreceptor function is altered by stress exposure leading to the observed increase in NE release, we perfused the slices with the selective  $\alpha_2$ -AR antagonist idazoxan (IDA). In classic *ex vivo* preparations with a single pulse stimulus, antagonists are often ineffective at altering catecholamine release due to lack of catecholamine tone within the slice. Optogenetic stimulation, however, allows for investigations of pulse trains with varying frequencies<sup>29</sup>, and indeed, increases in NE release are not observed to the first 2 pulses of light of a 2 Hz stimulation, but only to subsequent pulses (Fig 4A inset.). Therefore, optogenetic stimulation is ideal for using antagonists to monitor autoreceptor functions. In particular, it is advantageous to utilize an antagonist vs. an agonist, because antagonists theoretically would lead to an enhancement in the analyte vs. a reduction in the analyte. This provides us with enhanced confidence in our electrochemical recordings, as multiple factors can contribute to a “run down” in the electrochemical signal. To assess the role of  $\alpha_2$ -ARs following stress, we optically stimulated across a range of frequencies (1, 2, 5, 10, and 15 Hz, 20 pulses) at baseline, and then applied 10  $\mu$ M IDA and assessed the same range of optical stimulations. In both naïve and single stress exposed mice, IDA significantly increased NE release (Fig. 4A and 4B). Following repeated restraint stress, however,  $\alpha_2$ -antagonism failed to alter subsequent NE release (Fig. 4C). Whereas these data may be interpreted as a potential ceiling effect of NE release, we find higher concentrations available for release at higher frequencies, indicating the availability of additional NE for release. Therefore, we interpret these data to suggest that a loss in sensitivity at the  $\alpha_2$ -autoreceptor may underlie increased release of NE in mice that have experienced chronic stress. Furthermore, these data are consistent with experiments conducted in rat examining how morphine withdrawal and social isolation stress regulate NE release<sup>17-18</sup>, suggesting that this may be a common mechanism to elevate NE levels across species following traumatic stress.

The alterations of noradrenergic release properties we have shown may illustrate important underlying neurobiological mechanisms of psychiatric disorders. We all experience stress to some degree in our daily lives, but the transition from “normal” stress to maladaptive stress likely alters neuronal systems. Our data here, indicate that one of these systems altered by repeated stress exposure is the noradrenergic system which shows greater response to optogenetic stimuli and less control by inhibitory autoreceptors. A greater understanding of how this transition occurs, such as the duration or intensities of stress exposures necessary to alter NE function, the persistence of this effect, and additional mechanisms that contribute to these adaptations (e.g. the role of endocannabinoid and opioid systems), are still needed to further enhance our knowledge of stress disorders. Furthermore, our data here show that the DBH::Cre(+/-)::Ai32(+/+) mouse will be a useful tool to continue to investigate these processes, both in terms of adaptation within the noradrenergic circuitry itself, and in the subsequent neural systems that are modulated by NE. Regardless, this elevated noradrenergic tone may relate to hyperarousal states in disorders such as PTSD<sup>4</sup>, altered affect<sup>1</sup>, and susceptibility for addiction<sup>3</sup>.

## Methods

### Animals and Housing.

Adult male and female mice were tested with sex counterbalanced across groups for all experiments. Selective expression of ChR2 in noradrenergic neurons was achieved by breeding a cross between DBH::Cre(+/-)::Ai32(+/+) mouse with a Ai32(+/+) mouse. Mice were housed with littermates in a temperature-controlled vivarium with a 12:12 h light-dark cycle with lights on at 0700 h, and had *ad libitum* access to food and water. All procedures were approved by the Institutional Animal Care and Use Committee of the University of North Carolina at Chapel Hill.

### Stress Procedures.

Mice were placed in custom in-house modified ventilated 50 mL conical tubes for 2 h. Mice in the single stress exposure condition were tested the day following restraint. Mice in the repeated stress exposure condition were underwent restraint procedures for 2 h/day for 5 consecutive days. These mice were tested the day following the fifth restraint session.

### Corticosterone Analysis.

Mice were decapitated following restraint stress or from homecage (at 12:00 pm) and trunk blood was collected into heparinized tubes. Blood samples were immediately centrifuged (2000 x g for 10 minutes), plasma was isolated, placed on dry ice, and stored at -80°C until analysis. Plasma was analyzed for corticosterone content using a commercially available colorimetric ELISA kit (Arbor Assays; Ann Arbor, MI), according to the manufacturer's instructions. All samples were run in duplicate.

### Double Fluorescent *In Situ* Hybridization (FISH).

Brains were rapidly removed and flash frozen on dry ice for a minimum of 5 minutes, and then stored at -80 °C for no more than 1 week prior to slicing. Sections were then sliced on a cryostat (Leica 300s, Germany) at 18 μm and directly mounted onto slides and stored at

–80 °C prior to the FISH procedure. FISH was performed using the RNAScope kit (ACD Biotechnique) according to the manufacturer's instructions (except the time for protease IV step was reduced to 15 min) using antisense probes against *Dbh* (Mm-Dbh-C2 400921-C2) and *cFos* (Mm-Fos-C3 316921-C3). Sections were imaged on a Zeiss 800 confocal microscope using identical settings.

### **Slice Preparation, Electrophysiology, and Electrochemistry Recordings.**

Mice were deeply anesthetized (isoflurane), decapitated, and brains were harvested and placed in ice-cold sucrose for slicing (ACSF in mM: 194 sucrose, 20 NaCl, 4.4 KCl, 2 CaCl<sub>2</sub>, 1 MgCl<sub>2</sub>, 1.2 NaH<sub>2</sub>PO<sub>4</sub>, 10 glucose, 26 NaHCO<sub>3</sub>) that had been oxygenated with 95% O<sub>2</sub>, 5% CO<sub>2</sub> for at least 15 min. Brains were sliced at 300 μm using a Leica VT1000 (Germany). Following slicing, brains were incubated in oxygenated ACSF (in mM: 124 NaCl, 4.4 KCl, 2 CaCl<sub>2</sub>, 1.2 MgSO<sub>4</sub>, 1 NaH<sub>2</sub>PO<sub>4</sub>, 10 glucose, 26 NaHCO<sub>3</sub>, 34° C) and allowed to incubate for at least 30 minutes. Slices were transferred to the electrophysiology or electrochemistry rigs for patch clamp or fast scan cyclic voltammetry, respectively. Each rig perfused oxygenated ACSF (28–30 °C) through the bath at 2 ml/min. Cells expressing ChR2-eYFP were acquired using whole-cell voltage clamp and then switched to current-clamp mode (in mM: 135 gluconic acid-potassium, 5 NaCl, 2 MgCl<sub>2</sub>, 10 HEPES, 0.6 EGTA, 4 Na<sub>2</sub>ATP, 0.4 Na<sub>2</sub>GTP). Because NE neurons are spontaneously active, current was injected to keep the membrane potential at –70 mV and 10, 5 ms light pulses were applied with varying frequency (1, 2, 5, 10, and 15 Hz.) Electrochemical recordings were made as described previously<sup>30</sup>. Carbon fiber microelectrodes were fabricated in house with fiber lengths 50–100 μm. Electrodes were calibrated in ACSF with 3 concentrations of NE: 0.1 μM, 1.0 μM, and 10 μM NE. By graphing the peak current induced by each concentration of NE, we could draw a line of best fit whose slope was used as the current-concentration calibration factor for that electrode. The average calibration for all electrodes used in these experiments was 7.97 + 0.62 μM/1 nA (n=5). Using a custom built potentiostat (University of Washington, Seattle) and TarHeel CV written in laboratory view (National Instruments), a triangular waveform (–0.4 V to 1.3 V) was applied at 10 Hz. Slices were optically stimulated with 5-ms blue (490 nm) light pulses down the submerged 40x objective. Stimulation parameters included single pulse; 2, 5, 10, 20 pulses at either 5 Hz or 10 Hz; and 20 pulses at 1, 2, 5, 10, and 15 Hz. Each recording began with 2 s (20 voltammograms) of recording before stimulus delivery. Recordings were separated by >5 min. Voltammograms were analyzed with HDCV (UNC Chapel Hill) with NE currents isolated using principal component regression analysis where score plot and K-matrix CVs were compiled to determine the quality of the analysis, as described previously<sup>31</sup>, and [NE]<sub>max</sub> was determined with Clampfit 10.6 software (Molecular Devices, Sunnyvale, CA). 10 μM idazoxan (Sigma-Adrich, St Louis, MO) in ACSF was bath applied for >10 min before testing.

### **Data Analysis and Statistics.**

Data were analyzed using GraphPad Prism 7.0 and are represented as mean ± SEM. CORT comparisons and % of *Dbh*<sup>+</sup> cells expressing *cFos* were conducted using a one-way ANOVA. Between subjects (Figure 3) and within subjects (Figure 4) two-way ANOVAs were performed on all NE release analyses with repeated factors of Frequency (Fig. 3A

and4A) or Number of Light Pulses (Fig. 3B and C; 4B and C) and drug treatment (Fig. 4). Tukey's or Sidak's post hoc tests were conducted where appropriate. Significant differences were represented at \* $p < 0.05$ , \*\* $p < 0.05$ , \*\*\* $p < 0.005$ , and \*\*\*\* $p < 0.0001$ .

## Acknowledgements.

The authors would like to thank Dr. Patricia Jensen for generating and providing the DBH::Cre mice for these experiments. We also thank the Hooker Imaging Core at UNC and support from the Bowles Center for Alcohol Studies at UNC. We would like to thank Dr. Thomas Kash for comments on a previous version of the manuscript.

Funding Sources.

This research was funded by NIAAA grants: K01AA023555, U01AA020911, U24AA025475, R01AA019454, R01AA026537, F32AA026485, and T32AA007573. NINDS grant: T32NS007431

## Abbreviations.

<b>ACSF</b>	artificial cerebrospinal fluid
<b>BNST</b>	bed nucleus of the stria terminalis
<b>ChR2</b>	channelrhodopsin
<b>CORT</b>	corticosterone
<b>FSCV</b>	fast-scan cyclic voltammetry
<b>NE</b>	norepinephrine

## References

- Morilak DA; Barrera G; Echevarria DJ; Garcia AS; Hernandez A; Ma S; Petre CO, Role of brain norepinephrine in the behavioral response to stress. *Prog Neuropsychopharmacol Biol Psychiatry* 2005, 29 (8), 1214–24. [PubMed: 16226365]
- Schmidt KT; Weinshenker D, Adrenaline rush: the role of adrenergic receptors in stimulant-induced behaviors. *Mol Pharmacol* 2014, 85 (4), 640–50. [PubMed: 24499709]
- Weinshenker D; Schroeder JP, There and back again: a tale of norepinephrine and drug addiction. *Neuropsychopharmacology* 2007, 32 (7), 1433–51. [PubMed: 17164822]
- Southwick SM; Bremner JD; Rasmusson A; Morgan CA 3rd; Arnsten A; Charney DS, Role of norepinephrine in the pathophysiology and treatment of posttraumatic stress disorder. *Biol Psychiatry* 1999, 46 (9), 1192–204. [PubMed: 10560025]
- Foote SL; Bloom FE; Aston-Jones G, Nucleus locus ceruleus: new evidence of anatomical and physiological specificity. *Physiol Rev* 1983, 63 (3), 844–914. [PubMed: 6308694]
- Moore RY; Bloom FE, Central catecholamine neuron systems: anatomy and physiology of the norepinephrine and epinephrine systems. *Annu Rev Neurosci* 1979, 2, 113–68. [PubMed: 231924]
- Robertson SD; Plummer NW; de Marchena J; Jensen P, Developmental origins of central norepinephrine neuron diversity. *Nat Neurosci* 2013, 16 (8), 1016–23. [PubMed: 23852112]
- Woulfe JM; Flumerfelt BA; Hryciyshyn AW, Efferent connections of the A1 noradrenergic cell group: a DBH immunohistochemical and PHA-L anterograde tracing study. *Exp Neurol* 1990, 109 (3), 308–22. [PubMed: 1976532]
- Banihashemi L; Rinaman L, Noradrenergic inputs to the bed nucleus of the stria terminalis and paraventricular nucleus of the hypothalamus underlie hypothalamic-pituitary-adrenal axis but not hypophagic or conditioned avoidance responses to systemic yohimbine. *J Neurosci* 2006, 26 (44), 11442–53. [PubMed: 17079674]

10. Forray MI; Gysling K, Role of noradrenergic projections to the bed nucleus of the stria terminalis in the regulation of the hypothalamic-pituitary-adrenal axis. *Brain Res Brain Res Rev* 2004, 47 (1–3), 145–60. [PubMed: 15572169]
11. Park J; Kile BM; Wightman RM, In vivo voltammetric monitoring of norepinephrine release in the rat ventral bed nucleus of the stria terminalis and anteroventral thalamic nucleus. *Eur J Neurosci* 2009, 30 (11), 2121–33. [PubMed: 20128849]
12. Phelix CF; Liposits Z; Paull WK, Catecholamine-CRF synaptic interaction in a septal bed nucleus: afferents of neurons in the bed nucleus of the stria terminalis. *Brain Res Bull* 1994, 33 (1), 109–19. [PubMed: 7903902]
13. Ch'ng S; Fu J; Brown RM; McDougall SJ; Lawrence AJ, The intersection of stress and reward: BNST modulation of aversive and appetitive states. *Prog Neuropsychopharmacol Biol Psychiatry* 2018.
14. Cecchi M; Khoshbouei H; Javors M; Morilak DA, Modulatory effects of norepinephrine in the lateral bed nucleus of the stria terminalis on behavioral and neuroendocrine responses to acute stress. *Neuroscience* 2002, 112 (1), 13–21. [PubMed: 12044468]
15. McElligott ZA; Klug JR; Nobis WP; Patel S; Grueter BA; Kash TL; Winder DG, Distinct forms of Gq-receptor-dependent plasticity of excitatory transmission in the BNST are differentially affected by stress. *Proc Natl Acad Sci U S A* 2010, 107 (5), 2271–6. [PubMed: 20133871]
16. Nobis WP; Kash TL; Silberman Y; Winder DG, beta-Adrenergic receptors enhance excitatory transmission in the bed nucleus of the stria terminalis through a corticotrophin-releasing factor receptor-dependent and cocaine-regulated mechanism. *Biol Psychiatry* 2011, 69 (11), 1083–90. [PubMed: 21334600]
17. Fox ME; Studebaker RI; Swofford NJ; Wightman RM, Stress and Drug Dependence Differentially Modulate Norepinephrine Signaling in Animals with Varied HPA Axis Function. *Neuropsychopharmacology* 2015, 40 (7), 1752–61. [PubMed: 25601230]
18. McElligott ZA; Fox ME; Walsh PL; Urban DJ; Ferrel MS; Roth BL; Wightman RM, Noradrenergic synaptic function in the bed nucleus of the stria terminalis varies in animal models of anxiety and addiction. *Neuropsychopharmacology* 2013, 38 (9), 1665–73. [PubMed: 23467277]
19. Miles PR; Mundorf ML; Wightman RM, Release and uptake of catecholamines in the bed nucleus of the stria terminalis measured in the mouse brain slice. *Synapse* 2002, 44 (3), 188–97. [PubMed: 11954051]
20. Xu F; Gainetdinov RR; Wetsel WC; Jones SR; Bohn LM; Miller GW; Wang YM; Caron MG, Mice lacking the norepinephrine transporter are supersensitive to psychostimulants. *Nat Neurosci* 2000, 3 (5), 465–71. [PubMed: 10769386]
21. Madisen L; Mao T; Koch H; Zhuo JM; Berenyi A; Fujisawa S; Hsu YW; Garcia AJ 3rd; Gu X; Zanella S; Kidney J; Gu H; Mao Y; Hooks BM; Boyden ES; Buzsaki G; Ramirez JM; Jones AR; Svoboda K; Han X; Turner EE; Zeng H, A toolbox of Cre-dependent optogenetic transgenic mice for light-induced activation and silencing. *Nat Neurosci* 2012, 15 (5), 793–802. [PubMed: 22446880]
22. Herr NR; Park J; McElligott ZA; Belle AM; Carelli RM; Wightman RM, In vivo voltammetry monitoring of electrically evoked extracellular norepinephrine in subregions of the bed nucleus of the stria terminalis. *J Neurophysiol* 2012, 107 (6), 1731–7. [PubMed: 22190618]
23. O'Neill B; Patel JC; Rice ME, Characterization of Optically and Electrically Evoked Dopamine Release in Striatal Slices from Digenic Knock-in Mice with DAT-Driven Expression of Channelrhodopsin. *ACS Chem Neurosci* 2017, 8 (2), 310–319. [PubMed: 28177213]
24. Barnum CJ; Blandino P Jr.; Deak T, Adaptation in the corticosterone and hyperthermic responses to stress following repeated stressor exposure. *J Neuroendocrinol* 2007, 19 (8), 632–42. [PubMed: 17620105]
25. Rademacher DJ; Meier SE; Shi L; Ho WS; Jarrahian A; Hillard CJ, Effects of acute and repeated restraint stress on endocannabinoid content in the amygdala, ventral striatum, and medial prefrontal cortex in mice. *Neuropharmacology* 2008, 54 (1), 108–16. [PubMed: 17675104]
26. Brown E; Moehlis J; Holmes P; Clayton E; Rajkowski J; Aston-Jones G, The influence of spike rate and stimulus duration on noradrenergic neurons. *J Comput Neurosci* 2004, 17 (1), 13–29. [PubMed: 15218351]



27. Devilbiss DM; Waterhouse BD, Phasic and tonic patterns of locus coeruleus output differentially modulate sensory network function in the awake rat. *J Neurophysiol* 2011, 105 (1), 69–87. [PubMed: 20980542]
28. Saphier D, Catecholaminergic projections to tuberoinfundibular neurones of the paraventricular nucleus: I. Effects of stimulation of A1, A2, A6 and C2 cell groups. *Brain Res Bull* 1989, 23 (6), 389–95. [PubMed: 2611683]
29. McElligott Z, Optogenetic and Chemogenetic Approaches To Advance Monitoring Molecules. *ACS Chem Neurosci* 2015, 6 (7), 944–7. [PubMed: 25791746]
30. Li C; Sugam JA; Lowery-Gionta EG; McElligott ZA; McCall NM; Lopez AJ; McKlveen JM; Pleil KE; Kash TL, Mu Opioid Receptor Modulation of Dopamine Neurons in the Periaqueductal Gray/Dorsal Raphe: A Role in Regulation of Pain. *Neuropsychopharmacology* 2016, 41 (8), 2122–32. [PubMed: 26792442]
31. Bucher ES; Brooks K; Verber MD; Keithley RB; Owesson-White C; Carroll S; Takmakov P; McKinney CJ; Wightman RM, Flexible software platform for fast-scan cyclic voltammetry data acquisition and analysis. *Anal Chem* 2013, 85 (21), 10344–53. [PubMed: 24083898]

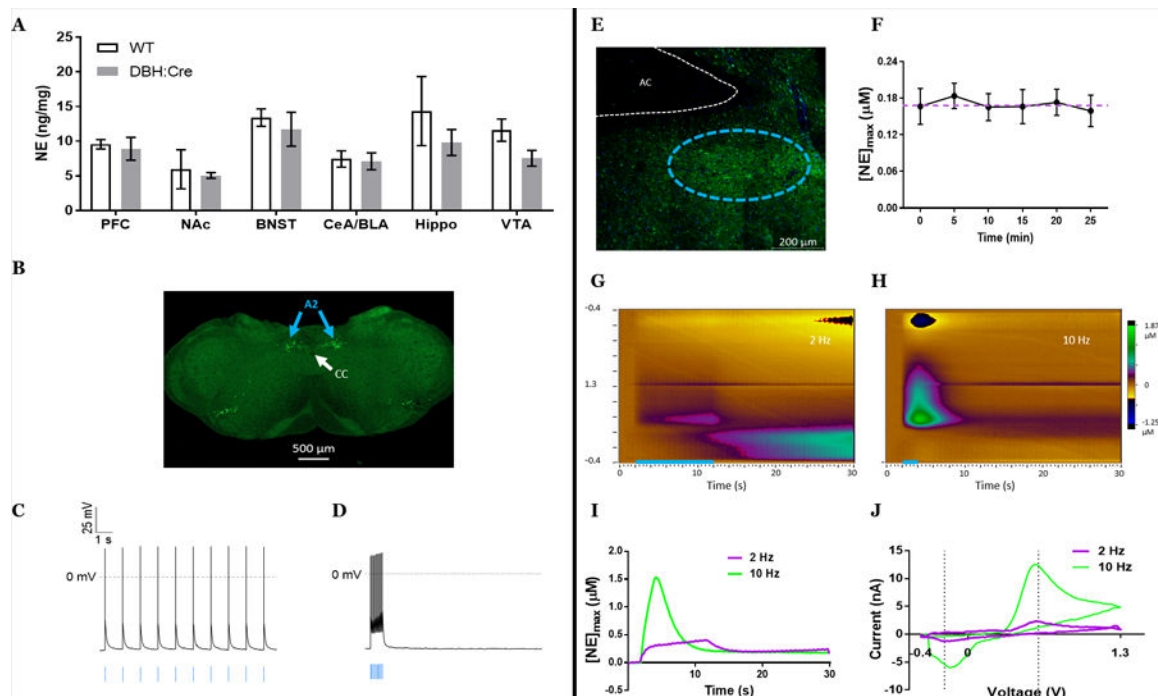


**Figure 1.**

DBH::Cre(+/-)::Ai32(+/+) mice act as a reliable model to study noradrenergic function. A) Transgene expression does not alter norepinephrine tissue content across multiple brain regions;  $p > 0.05$ . B) Cell body expression of GFP labeling noradrenergic neurons in the A2 cell group of the medullary nucleus of the solitary tract C,D) Patch clamp electrophysiology shows that GFP+ neurons in A2 fire action potentials in response to optogenetic cell body stimulation (blue bars) at both 1 Hz (C) and 15 Hz (D) frequencies. E) Terminal projections (green = GFP) in fusiform subnucleus (outlined in cyan dashes) of the ventral bed nucleus of the stria terminalis. F) 10 Hz, 20 pulse optogenetic stimulation of the vBNST induces consistent concentrations of norepinephrine release over multiple stimulations. Mean $\pm$ SEM;  $n = 4$  recording sites from 4 mice;  $p > 0.05$ . G) Color plot representing NE release following 2 Hz, 20 pulses of optogenetic stimulation. H) Color plot representing NE release following 10 Hz, 20 pulses of optogenetic stimulation. I) Representative norepinephrine concentration over time following either 2 Hz, 20 pulses pulse (lilac) or 10 Hz, 20 pulses (lime). Optogenetic stimulation occurred at 2 s. J) Representative cyclic voltammograms of either 2 Hz, 20 pulses pulse (lilac) or 10 Hz, 20 pulses (lime).

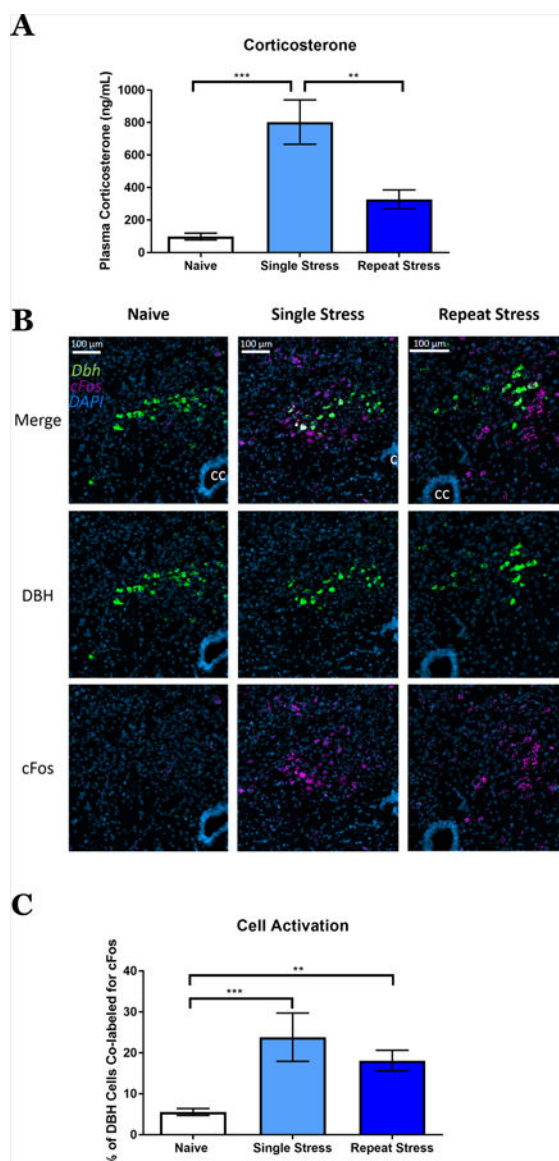


**Figure 2.** Immediate response of corticosterone and neuronal activation to restraint stress. A) Plasma corticosterone (ng/mL) from naïve, single stress, and repeat stress mice. Mean±SEM; n = 5–6 mice/group. One-way ANOVA ( $F = 15.07$ ,  $p < 0.001$ ). B) Nucleus of the solitary tract double fluorescent in situ hybridization showing DBH (green), cFos (lilac), and DAPI (blue) in stress naïve, single stress, and repeat stress mice. CC = central canal. C) Percent of DBH+ neurons that were colabeled for cFos. Mean±SEM; n = 4–8 mice/group. One-way ANOVA ( $F = 11.31$ ,  $p < 0.001$ ). \*\* $p < 0.05$ , \*\*\*  $p < 0.005$ .

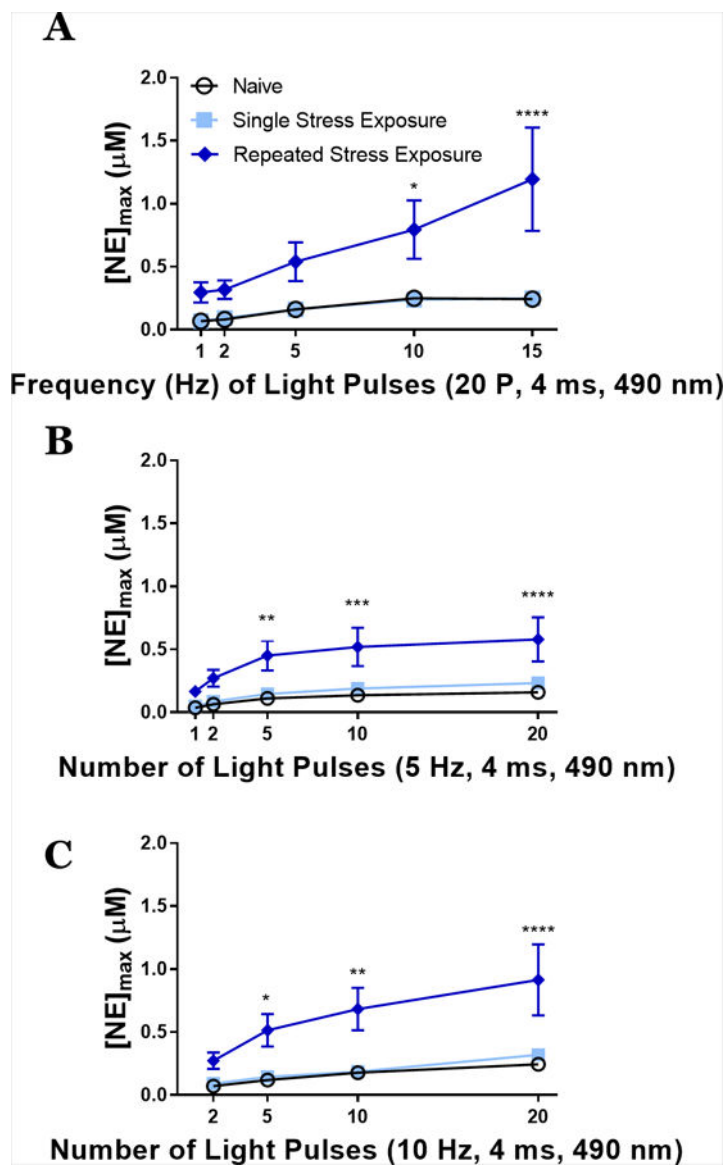


**Figure 3.** Repeated stress exposure increases norepinephrine release at multiple stimulation parameters. A) Varied frequencies of 20 pulse stimulations induce different peak concentrations of norepinephrine ( $[\text{NE}]_{\text{max}}$ ) between stress naïve, single stress exposed, and repeated stress exposed mice. Two-way repeated measures ANOVA, main effects of frequency ( $F = 7.66$ ,  $p < 0.0001$ ) and stress exposure ( $F = 7.733$ ,  $p = 0.004$ ) with a significant interaction ( $F = 2.484$ ,  $p = 0.0199$ ). B) Varied number of light pulses at 5 Hz stimulation induce different peak concentrations of norepinephrine between stress naïve, single stress exposed, and repeated stress exposed mice. Two-way repeated measures ANOVA, main effects of frequency ( $F = 23.01$ ,  $p < 0.0001$ ) and stress exposure ( $F = 7.37$ ,  $p = 0.004$ ) with a significant interaction ( $F = 3.229$ ,  $p = 0.0031$ ). C) Varied number of light pulses at 10 Hz stimulation induce different peak concentrations of norepinephrine between stress naïve, single stress exposed, and repeated stress exposed mice. Two-way repeated

measures ANOVA, main effects of frequency ( $F = 21.27$ ,  $p < 0.0001$ ) and stress exposure ( $F = 8.09$ ,  $p = 0.0027$ ) with a significant interaction ( $F = 3.721$ ,  $p = 0.0033$ ). Mean $\pm$ SEM;  $n = 7$ – $8$  slices/group from  $5$ – $6$  mice/group. \* $p < 0.05$ , \*\* $p < 0.05$ , \*\*\*  $p < 0.005$ , and \*\*\*\* $p < 0.0001$ .

Author Manuscript

Author Manuscript

Author Manuscript

Author Manuscript

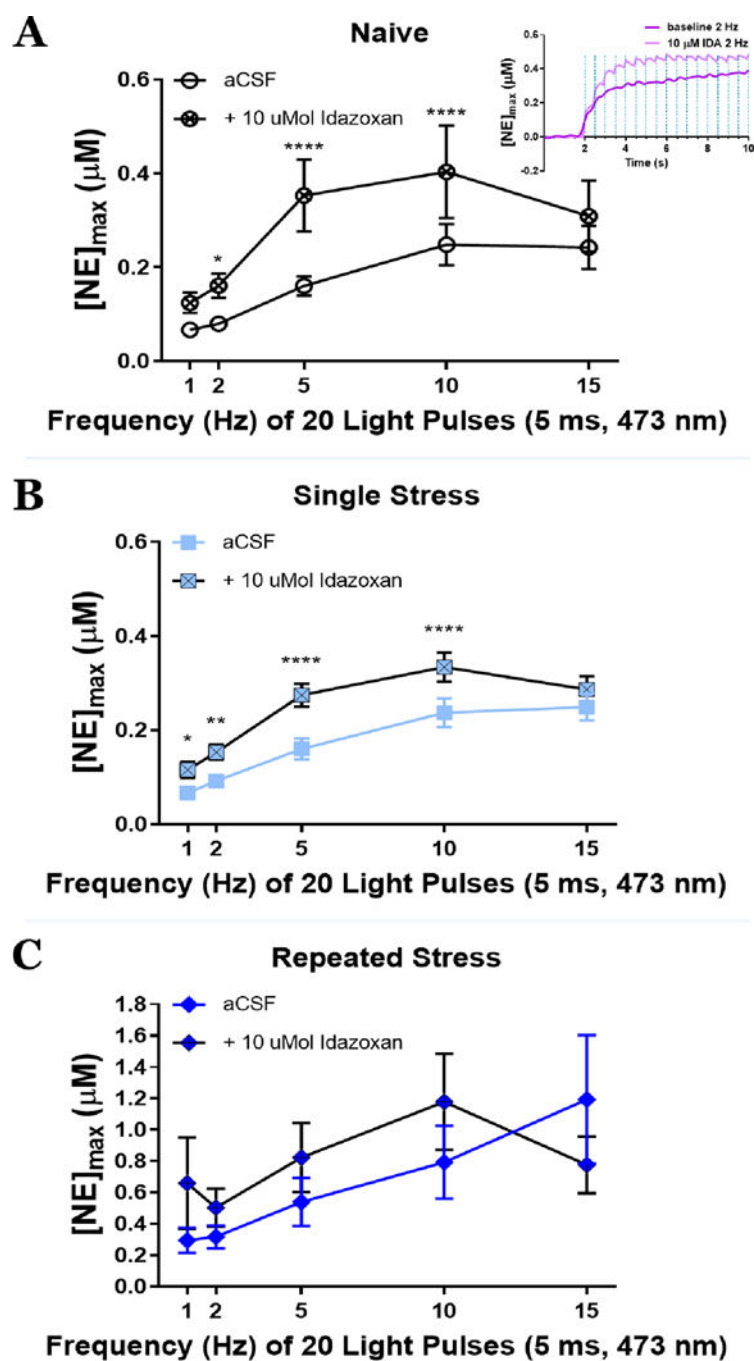


**Figure 4.** The  $\alpha_2$ -adrenergic autoreceptor antagonist, idazoxan (10  $\mu$ Mol) effect on peak concentrations of norepinephrine ([NE]<sub>max</sub>). A) idazoxan increases NE peak in stress naïve mice,  $F = 11.05$ ,  $p = 0.02$ ; inset: initial changes in NE following idazoxan within a 2 Hz pulse train. B) increases peak concentrations of norepinephrine single stress exposed mice,  $F = 74.18$ ,  $p = 0.0001$ . C) Idazoxan fails to increase NE concentrations following repeated

stress,  $p > 0.05$ . aCSF = artificial cerebrospinal fluid. Mean $\pm$ SEM; n = 6–7 slices/group from 5–6 mice/group. \* $p < 0.05$ , \*\* $p < 0.05$ , \*\*\*  $p < 0.005$ , and \*\*\*\* $p < 0.0001$ .

Author Manuscript

Author Manuscript

Author Manuscript

Author Manuscript